

## **APPROACH TO PROVE THE EFFICIENCY OF THE MONTE CARLO METHOD COMBINED WITH THE ELEMENTARY EFFECT METHOD TO QUANTIFY UNCERTAINTY OF A BEAM STRUCTURE WITH PIEZO-ELASTIC SUPPORTS**

**Sushan Li<sup>1</sup>, Benedict Götz<sup>1</sup>, Maximilian Schaeffner<sup>1</sup>, and Roland Platz<sup>2</sup>**

<sup>1</sup> Research group System Reliability, Adaptive Structures, and Machine Acoustics SAM  
TU Darmstadt  
Magdalenenstr. 4, Darmstadt, Germany  
e-mail: {sLi, goetz, schaeffner}@sam.tu-darmstadt.de

<sup>2</sup> Fraunhofer Institute for Structural Durability and System Reliability LBF  
Bartningstr. 47, Darmstadt, Germany  
e-mail: roland.platz@lbf.fraunhofer.de

**Keywords:** Uncertainty quantification, Monte Carlo method, Elementary Effect method, beam, piezo-elastic support

**Abstract.** *In this paper, a new approach is presented to prove the efficiency of the direct Monte Carlo method combined with the Elementary Effect method to quantify structural data uncertainty under uncertain input parameters of a beam structure. Normally, the application of the direct Monte Carlo method requires high computational cost when all input parameters are taken into account. It is proposed to use a combination of the direct Monte Carlo method and the Elementary Effect method for the variance-based sensitivity analysis, named the combined Monte Carlo method. By the application of the Elementary Effect method as a screening method, the truly influential input parameters are identified. Then, the parametric uncertainty is analyzed only under these influential input parameters' uncertainty by the use of the Monte Carlo method. Through a combination of these two methods, the number of simulations can be significantly reduced due to the reduction of the number of analyzed input parameters.*

*The novelty of this paper is to investigate the accuracy and the efficiency of this combined approach by the use of a beam structure with piezo-elastic supports for buckling and vibration control as a reference structure. The uncertain structural input parameters are the geometric, material, and stiffness parameters of the piezo-elastic supports. The output variable is the first lateral resonance frequency of the beam structure. Its uncertainty will be analyzed by the application of the combined Monte Carlo method applied for only a few but influential input parameters and will also be analyzed by the application of the direct Monte Carlo method for all input parameters. The results by the two methods will be compared based on the analysis accuracy to estimate the sensitivity of the input parameters on the first lateral resonance frequency and the minimal required number of the simulations.*

## 1 INTRODUCTION

Global sensitivity analysis shows how the uncertainty of a structure is apportioned to the uncertainty of its input parameters by quantifying the relative importance of each input parameter [1]. The underlying goal of the sensitivity analysis is to identify the influential input parameters and then, through controlling and reducing the uncertainty of the influential input parameters, to reduce the uncertainty of the structure [2], e.g., to reduce the uncertainty of the structural vibration amplitude.

The methods that are used for global sensitivity analysis can be divided into two categories, the qualitative analysis methods and the quantitative analysis methods [2]. The qualitative analysis methods, also named screening methods, are feasible to identify if the input parameters have relevant influence on the structure or not [3]. Commonly, they identify the relevant influence based on a small number of simulations. In most cases, “a small number” implies that the simulations do not result in convergence or trustworthy outcomes. Similarly, “a relatively large number” implies that the simulations do converge and trustworthy outcomes are reached, but usually with high costs in simulation time. Therefore, a small number of simulations in the qualitative analysis is commonly not sufficient for ranking the relevant influence of the input parameters on the structure. In contrast, the quantitative analysis methods aim at precisely quantifying and ranking the influence of the input parameters on the structure, based on a relatively large number of simulations [3]. Hence, an approach by combination of the qualitative and the quantitative analysis method can be an efficient approach in sensitivity analysis.

The global sensitivity analysis methods are classified in terms of required number of simulations and the structure’s complexity in [2]. Based on this classification it can be concluded that the Elementary Effect method, which was proposed by Morris in 1991 [4], is a simple but effective screening method [5]. The studies in [6, 7] also support this statement. In the category of the quantitative analysis methods, the Monte Carlo method for variance-based sensitivity analysis is more feasible than other methods, e.g., the Fourier Amplitude Sensitivity Test (FAST), as it requires no assumption and considers not only the linear relation between the input parameters and output variable but also the nonlinear relation [8]. The studies in [9, 10] also support this statement. In this study, the Elementary Effect method is applied at first for screening the sensitivity of each input parameter to identify the input parameters having dynamic influence on the structure. Based on the screening results, the parametric uncertainty is analyzed only under the uncertainty of the influential input parameters by the Monte Carlo method for variance-based sensitivity analysis. The idea of the combination of these two methods is to reduce the number of simulations without losing the accuracy of the uncertainty analysis. This approach was recommended by Saltelli in [5]. The efficiency of this approach will be tested on a real beam structure subject to buckling and vibration control under axial loading with piezo-elastic supports

The beam structure is described in section 2 and modeled mathematically in section 3. The Elementary Effect method, the direct Monte Carlo method, and the combined Monte Carlo method are introduced in section 4. The Elementary Effect method is applied to the beam structure and the screening results are described in section 5. The sensitivity analysis results of the beam structure based on the direct Monte Carlo method and the combined Monte Carlo method are also described and compared in section 5 with respect to their analysis accuracy and computational costs. The goal of this paper is to investigate if the efficiency of the quantification of uncertainty is improved through the combination of the sensitivity analysis methods without losing the accuracy of the uncertainty analysis.

## 2 STRUCTURE DESCRIPTION

The reference structure for the application of the global sensitivity analysis is a beam with piezo-elastic supports that is used for two different applications of passive and active structural control: active buckling control [11] and passive lateral vibration attenuation [12]. Figure 1 shows the beam structure with piezo-elastic supports and the sectional view of the piezo-elastic support. It consists of a membrane-like spring element, an axial extension of the beam, and two piezoelectric stack transducers, which are mechanically prestressed by a stack of disc springs [13].

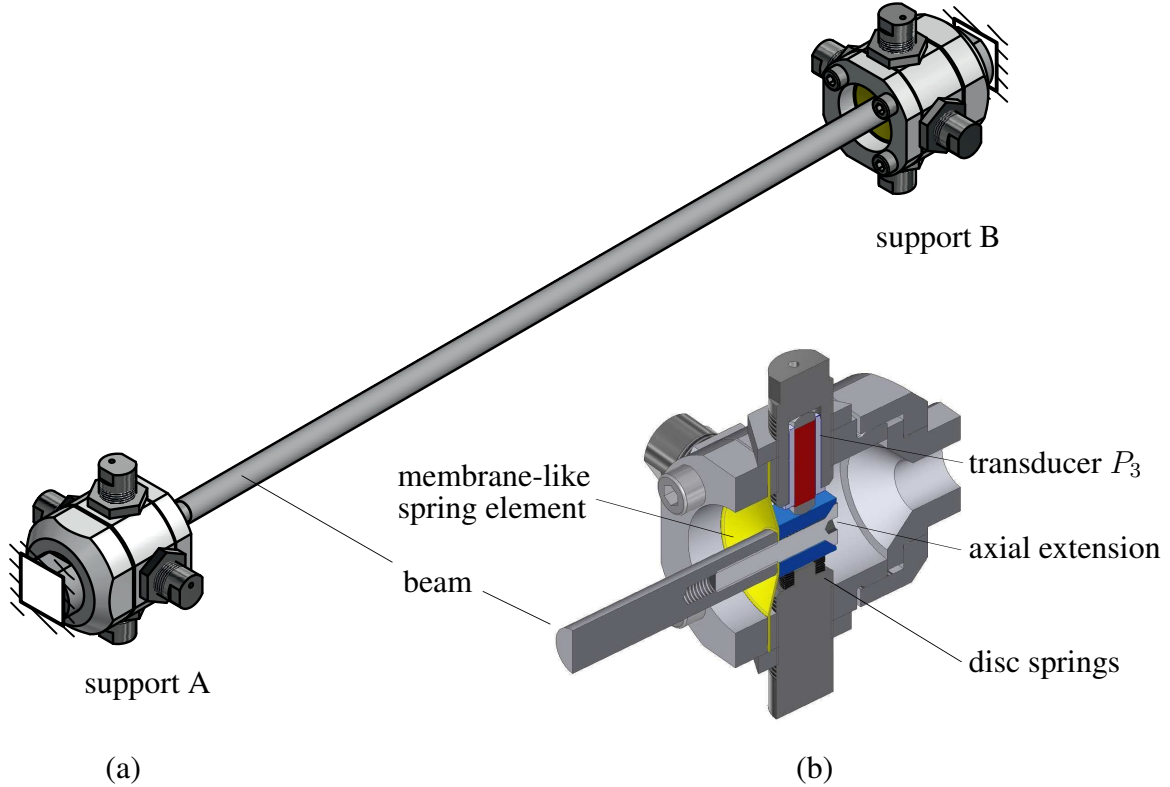


Figure 1: (a) CAD model of the beam with piezo-elastic supports, (b) Sectional view of piezo-elastic support B

The various components of the piezo-elastic supports may each influence the dynamic behavior of the beam structure. The input parameters of the piezo-elastic supports that have significant influence on the dynamic behavior of the beam structure will be identified. The first lateral resonance frequency  $f_1$  is an important measure for active buckling control and passive lateral vibration attenuation. Therefore, it is chosen as the output variable in this study for the global sensitivity analysis.

The mechanical sketch of the beam structure with piezo-elastic supports is shown in Figure 2. The beam is made of aluminum alloy EN AW-7075 with Young's modulus  $E_b$ , density  $\rho_b$ , length  $l_b$ , and circular solid cross-section of radius  $r_b$ . The circumferential lateral stiffness is homogeneous and has no preferred direction of lateral deflection, so the beam may deflect in any plane lateral to the longitudinal  $x$ -axis.

Two piezo-elastic supports A and B are located at  $x = 0$  mm and  $x = l_b$ . The elastic membrane-like spring elements made of spring steel 1.1248 in both supports A and B are represented by lateral stiffness  $k_{y,A} = k_{z,A} = k_{l,A}$  and  $k_{y,B} = k_{z,B} = k_{l,B}$  in  $y$ - and  $z$ -direction and

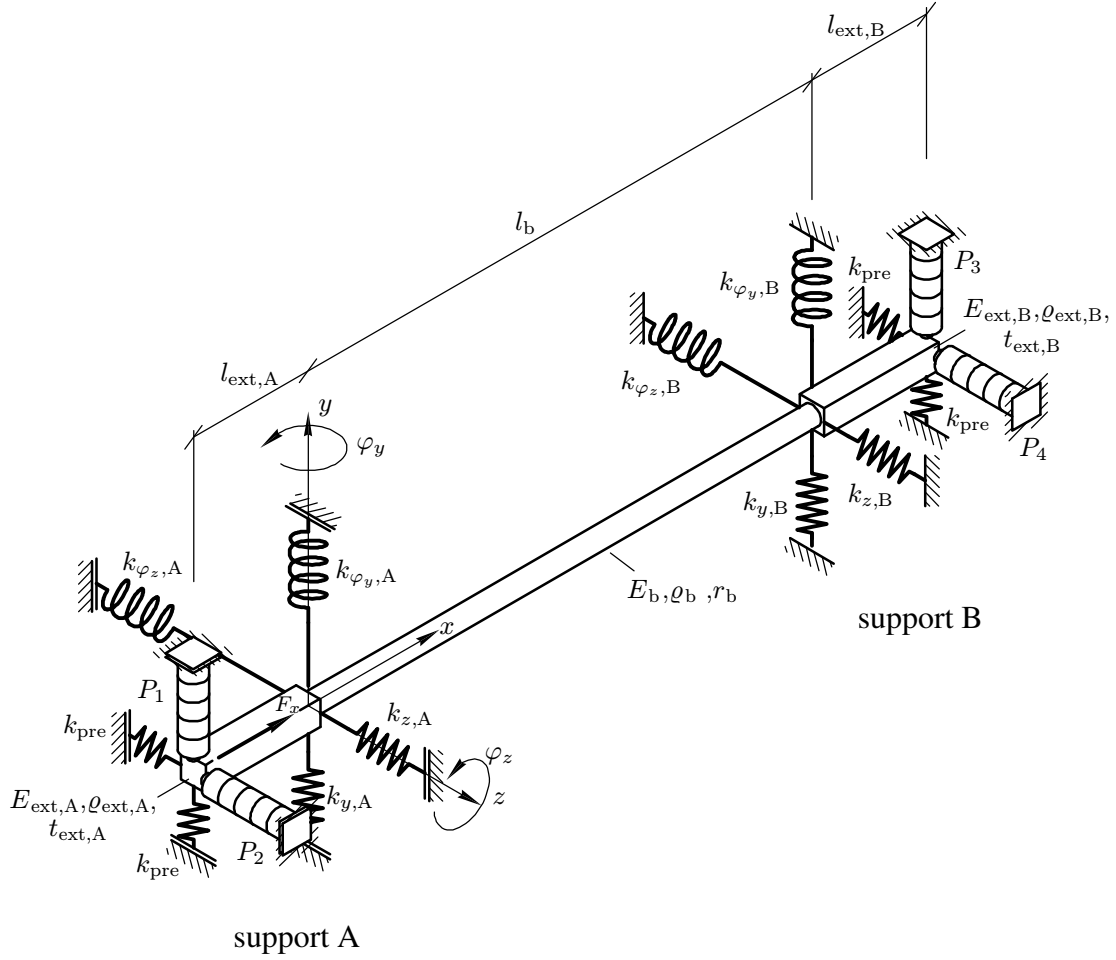


Figure 2: Simplified model of the beam structure with piezo-elastic supports A and B [12]

rotational stiffness  $k_{\varphi_y,A} = k_{\varphi_z,A} = k_{r,A}$  and  $k_{\varphi_y,B} = k_{\varphi_z,B} = k_{r,B}$  around the  $y$ - and  $z$ -axes. The spring stiffness values are assumed to be equal in  $y$ - and  $z$ -direction for this study since both directions are modeled symmetric and independent of each other. The spring element stiffness values are obtained from experimental static load measurements.

In each piezo-elastic support A and B at  $x = -l_{\text{ext}}$  and  $x = l_b + l_{\text{ext}}$ , two piezoelectric stack transducers  $P_1$  and  $P_2$  as well as  $P_3$  and  $P_4$  are arranged in the support housing at an angle of  $90^\circ$  to each other orthogonal to the beam's  $x$ -axis, Figure 2. All transducers are mechanically prestressed by a stack of disc springs with stiffness  $k_{\text{pre}}$ . The value of  $k_{\text{pre}}$  is smaller than 5% of the stiffness of the piezoelectric transducers. Therefore, its influence is neglected in this study. The transducers in supports A and B are connected to the beam via relatively stiff axial extensions made of hardened steel 1.2312 with Young's moduli  $E_{\text{ext},A}$  and  $E_{\text{ext},B}$ , densities  $\varrho_{\text{ext},A}$  and  $\varrho_{\text{ext},B}$ , lengths  $l_{\text{ext},A}$  and  $l_{\text{ext},B}$ , as well as edge lengths  $t_{\text{ext},A}$  and  $t_{\text{ext},B}$ . With that, lateral beam deflections in  $y$ - and  $z$ -direction are transformed into the stack transducer's axial deformation in  $y$ - and  $z$ -direction and vice versa. The piezoelectric transducers  $P_1$  and  $P_2$  in support A and  $P_3$  and  $P_4$  in support B are P-885.51 stack transducers by *PI Ceramic* with mechanical stiffness  $k_{p,A}$  and  $k_{p,B}$  [12].

The sensitivity analysis identifies the input parameters of the piezo-elastic supports that have significant influence on the first lateral natural frequency of the beam structure. For that, only the geometric and material properties of the beam,  $E_b, \rho_b, l_b, r_b$ , are constant, Table 1. The

geometric, material, and stiffness parameters of the components in the piezo-elastic supports are assumed uncertain parameters  $p_k$  with  $k = 1, 2, \dots, K = 14$ , Table 1. Their assumed normal or uniform distribution functions  $\mathcal{N}$  and  $\mathcal{U}$  are also given in Table 1. For the normal distribution function  $\mathcal{N}(\mu; \sigma)$ , the mean  $\mu$  and standard deviation  $\sigma$  are given and for the uniform distribution  $\mathcal{U}(\min; \max)$ , the minimum and maximum values are given.

Table 1: Geometric, material, and stiffness properties of the beam structure

input parameters		deterministic value	distribution function
$E_b$	beam Young's modulus in GPa	73.9	–
$\rho_b$	beam density in kg/m <sup>3</sup>	2 775	–
$l_b$	beam length in mm	400	–
$r_b$	beam radius in mm	5	–
$E_{\text{ext,A}}$	$p_1$ axial extension Young's modulus in GPa	210	$\mathcal{N}(210; 3.35)$
$\rho_{\text{ext,A}}$	$p_2$ extension density in kg/m <sup>3</sup>	7800	$\mathcal{N}(7800; 130)$
$l_{\text{ext,A}}$	$p_3$ extension length in mm	7.8	$\mathcal{U}(7.4; 8.2)$
$t_{\text{ext,A}}$	$p_4$ extension radius in mm	6	$\mathcal{U}(6; 6.1)$
$E_{\text{ext,B}}$	$p_5$ axial extension Young's modulus in GPa	210	$\mathcal{N}(210; 3.35)$
$\rho_{\text{ext,B}}$	$p_6$ extension density in kg/m <sup>3</sup>	7800	$\mathcal{N}(7800; 130)$
$l_{\text{ext,B}}$	$p_7$ extension length in mm	7.8	$\mathcal{U}(7.4; 8.2)$
$t_{\text{ext,B}}$	$p_8$ extension radius in mm	6	$\mathcal{U}(6; 6.1)$
$k_{l,A}$	$p_9$ spring lateral stiffness in N/m	$22 \cdot 10^6$	$\mathcal{N}(22 \cdot 10^6; 7.3 \cdot 10^5)$
$k_{r,A}$	$p_{10}$ spring rotational stiffness in N · m/rad	449.7	$\mathcal{N}(449.7; 30)$
$k_{l,B}$	$p_{11}$ spring lateral stiffness in N/m	$22 \cdot 10^6$	$\mathcal{N}(22 \cdot 10^6; 7.3 \cdot 10^5)$
$k_{r,B}$	$p_{12}$ spring rotational stiffness in N · m/rad	449.7	$\mathcal{N}(449.7; 30)$
$k_{p,A}$	$p_{13}$ piezo transducer A lateral stiffness in N/m	$49 \cdot 10^6$	$\mathcal{N}(49 \cdot 10^6; 3.3 \cdot 10^6)$
$k_{p,B}$	$p_{14}$ piezo transducer B lateral stiffness in N/m	$49 \cdot 10^6$	$\mathcal{N}(49 \cdot 10^6; 3.3 \cdot 10^6)$

Table 1 summarizes the constant and varied geometric, material, and stiffness properties for the following study. The input parameters relating to the axial extensions are  $p_1$ – $p_8$ . Due to the manufacturing tolerances the geometric properties  $p_3$ ,  $p_4$ ,  $p_7$ , as well as  $p_8$  are assumed uniformly distributed. The variation of the material properties  $p_1$ ,  $p_2$ ,  $p_5$ , and  $p_6$  are assumed normally distributed. Their distribution functions are defined according to the tolerance's specifications and material data found in literature. The input parameters describing the stiffness of the membrane-like spring elements are  $p_9$ – $p_{12}$ . The spring elements are produced by an actively controlled forming process. Thus, the variation of the spring stiffness properties are assumed to be normally distributed. Their distribution functions are defined according to the authors' static stiffness measurements. Finally, the lateral stiffnesses of the piezoelectric stack transducers are  $p_{13}$  and  $p_{14}$ . As they depend on the material properties, they are assumed normally distributed and their distribution functions are defined according to manufacturer data by *PI Ceramic* [14].

### 3 MATHEMATICAL MODEL

To calculate the first lateral resonance frequency  $f_1$  of the beam, a finite element (FE) model was derived in [11]. The free vibration of the beam with piezo-elastic supports in Figure 2 is modeled by the homogeneous FE equation of motion

$$\mathbf{M} \ddot{\mathbf{r}} + \mathbf{K} \mathbf{r} = 0. \quad (1)$$

Damping in equation (1) is neglected because it is insignificantly small according to the authors' experimental measurements. In equation (1),  $\mathbf{r}$  is the  $[4I \times 1]$  FE displacement vector for a beam discretized by  $(I - 1)$  elements with  $4I$  degrees of freedom, two translational and two rotational displacements in and around  $y$ - and  $z$ -direction.  $\mathbf{M}$  is the  $[4I \times 4I]$  mass matrix and  $\mathbf{K}$  is the  $[4I \times 4I]$  stiffness matrix. The discrete stiffness parameters of the elastic membrane springs, disk springs, and piezoelectric stack actuators are included in stiffness matrix  $\mathbf{K}$ .

The first lateral resonance frequency of the beam  $f_1$  is calculated by the solution of the characteristic equation

$$\det [\mathbf{K} - (2\pi f_1)^2 \mathbf{M}] = 0. \quad (2)$$

The influence of the  $K$  varied input parameters, which are contained in the  $[1 \times K]$  vector  $\mathbf{p} = [p_1, p_2, \dots, p_k, \dots, p_K]$  with  $k = 1, 2, \dots, K = 14$ , on the output parameter, which is the first lateral resonance frequency  $f_1$  in equation (2), will be identified by the sensitivity analysis.

## 4 METHODS FOR SENSITIVITY ANALYSIS

As already mentioned, the goal of this study is to prove the accuracy and the efficiency of the combination of the Elementary Effect method and the Monte Carlo method for the variance-based sensitivity analysis according to [5] for adequate sensitivity analysis. The Elementary Effect method, the direct Monte Carlo method for the variance-based sensitivity analysis, and the combined Monte Carlo method for the variance-based sensitivity analysis are briefly introduced in this section.

### 4.1 Screening method: the Elementary Effect method

The Elementary Effect method is a commonly used screening method as it can identify the influential input parameters of most structures [5]. After sampling and numerical simulations, the elementary effect of each input parameter is calculated. For analyzing a structure with  $K$  independent input parameters  $p_k$ ,  $k = 1, 2, \dots, K$ , which spans a  $K$ -dimensional input space  $\Omega^K$ , the Elementary Effect method identifies the input parameters having an influence on the output variable by comparing the mean and the standard deviation of the elementary effects of each input parameter.

For a structure with  $K$  input parameters, the sampling process for the Elementary Effect method begins by randomly choosing simulation points  $\mathbf{p}_{r,0} = [p_{r,0,1}, p_{r,0,2}, \dots, p_{r,0,K}]$  in  $\Omega^K$  with  $r = 0, 1, 2, \dots, R$ . These simulation points are used as base points and  $R$  represents the number of the base points used in the screening. Based on the base point  $\mathbf{p}_{r,0}$ , simulation points  $\mathbf{p}_{r,k} = [p_{r,k,1}, p_{r,k,2}, \dots, p_{r,k,K}]$  are generated by randomly varying the  $k$ -th input parameter for  $k = 1, 2, \dots, K$  inside  $\Omega^K$ . As the Elementary Effect method is used for parameter screening, it is suggested that the number of the base points  $R = 10$  is sufficient to produce valuable results [5].

The sampling process is illustrated by using a structure with only two input parameters  $K = 2$  as an example, Figure 3:

- For  $r = 1$ ,
  - Step 1.0: The first base point  $\mathbf{p}_{1,0}$  is randomly chosen in  $\Omega^K$ ,
  - Step 1.1: based on  $\mathbf{p}_{1,0}$ , the input parameter  $p_1$  is varied with a random length inside  $\Omega^K$  for the simulation point  $\mathbf{p}_{1,k} = \mathbf{p}_{1,1}$ ,

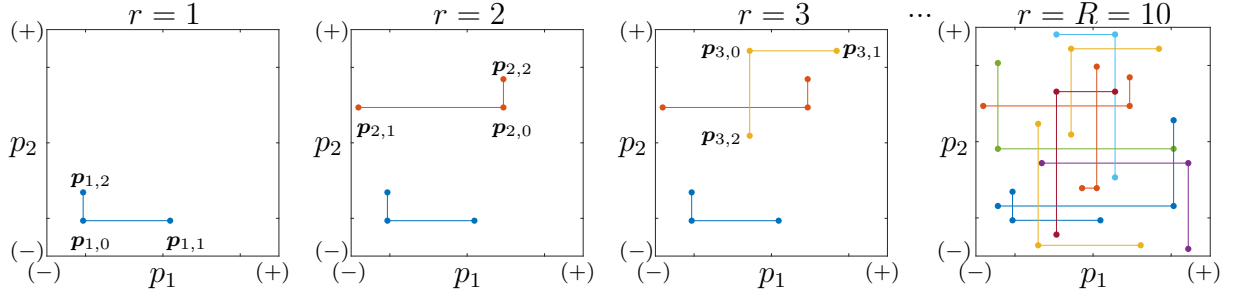


Figure 3: Sampling process by using the Elementary Effect method for a structure with two input parameters

Step 1.2: based on  $\mathbf{p}_{1,0}$ , the input parameter  $p_2$  is varied with a random length inside  $\Omega^K$  for the simulation point  $\mathbf{p}_{r,k} = \mathbf{p}_{1,2}$ ;

- For  $r = 2$ ,

Step 2.0: The second base point  $\mathbf{p}_{2,0}$  is randomly chosen in  $\Omega^K$ ,

Step 2.1: based on  $\mathbf{p}_{2,0}$ , the input parameter  $p_1$  is varied with a random length inside  $\Omega^K$  for the simulation point  $\mathbf{p}_{r,k} = \mathbf{p}_{2,1}$ ,

Step 2.2: based on  $\mathbf{p}_{2,0}$ , the input parameter  $p_2$  is varied with a random length inside  $\Omega^K$  for the simulation point  $\mathbf{p}_{r,k} = \mathbf{p}_{2,2}$ ;

- For  $r = 3$ ,

Step 3.0: The third base point  $\mathbf{p}_{3,0}$  is randomly chosen in  $\Omega^K$ ,

Step 3.1 and step 3.2: repeat the processes as in steps 1.1 and 1.2 but based on the third base point  $\mathbf{p}_{3,0}$ ;

- ... ;

- For  $r = R = 10$ ,

Step 10.0: The tenth base point  $\mathbf{p}_{10,0}$  is randomly chosen in  $\Omega^2$ , also the last base point,

Step 10.1 and step 10.2: repeat the processes as in steps 1.1 ... 1.2 but based on the tenth base point  $\mathbf{p}_{10,0}$ .

For a structure with  $K$  input parameters, based on each base point  $\mathbf{p}_{r,0}$ ,  $K$  simulation points  $\mathbf{p}_{r,1}, \mathbf{p}_{r,2}, \dots, \mathbf{p}_{r,K}$  are sampled. Hence, the number of simulations are  $N_{EE} = R \cdot (1 + K)$ . The function  $f(\mathbf{p})$  describes the relation between the input parameters  $\mathbf{p} = [p_1, p_2, \dots, p_K]$  and the output variable of the structure. Therefore, the results at the base points  $\mathbf{p}_{r,0}$  are  $f(\mathbf{p}_{r,0})$  and the results at the simulation points  $\mathbf{p}_{r,k}$  are  $f(\mathbf{p}_{r,k})$ . In this study the function  $f(\mathbf{p})$  is evaluated according to equations (2) with  $f(\mathbf{p}) = f_1$ . The simulations provide  $R \cdot K$  elementary effects  $EE_k^r$ ; one elementary effect per input parameter  $p_k$  based on each base point. The elementary effects  $EE_k^r$  of each input parameter are

$$EE_k^r = \frac{f(\mathbf{p}_{r,k}) - f(\mathbf{p}_{r,0})}{\Delta}, \quad (3)$$

$$\Delta = \frac{p_{r,k,k} - p_{r,0,k}}{p_{k,\max} - p_{k,\min}} \quad (4)$$

[5], with  $[1 \times K]$  simulation point vector  $\mathbf{p}_{r,k} = [p_{r,k,1}, p_{r,k,2}, \dots, p_{r,k,k}, \dots, p_{r,k,K}]$ ,  $[1 \times K]$  base point vector  $\mathbf{p}_{r,0} = [p_{r,0,1}, p_{r,0,2}, \dots, p_{r,0,k}, \dots, p_{r,0,K}]$ ,  $r = 1, 2, \dots, R$ , and  $k = 1, 2, \dots, K$ . The values of  $p_{k,\max}$  and  $p_{k,\min}$  represent the maximal and the minimal values of the  $k$ -th input parameter.

The distribution of the elementary effects  $EE_k^r$  for each input parameter is evaluated by the mean  $\hat{\mu}_k$  and the standard deviation  $\hat{\sigma}_k$  of the elementary effects  $EE_k^r$ . They are estimated as follows [5]:

$$\hat{\mu}_k = \frac{1}{R} \sum_{r=1}^R |EE_k^r|, \quad (5)$$

$$\hat{\sigma}_k = \sqrt{\frac{1}{R-1} \sum_{r=1}^R (EE_k^r - \hat{\mu}_k)^2}. \quad (6)$$

The mean  $\hat{\mu}_k$  of the elementary effect for the  $k$ -th input parameter is a sensitivity measure proposed to assess the overall influence of the  $k$ -th input parameter on the output variable [6]. A relatively high value of  $\hat{\mu}_k$  indicates that the  $k$ -th input parameter has a significant influence on the result of the calculated output variable. In contrast, a relatively low value of  $\hat{\mu}_k$  implies that the  $k$ -th input parameter has only minor influence on the result of the output variable.

Another measure is the standard deviation  $\hat{\sigma}_k$  of the elementary effect for the  $k$ -th input parameter, which estimates whether the effect of the  $k$ -th input parameter is linear or nonlinear or whether this input parameter has a interacted functional relation with other input parameters to calculate the output variable or not [4, 6]. In case the  $k$ -th input parameter's functional relation is linear, the elementary effects would be identical everywhere in the input space  $\Omega^K$ . Therefore,  $\hat{\sigma}_k$  is close to 0. In contrast, if the input parameter's functional relation is nonlinear and/or interacts with other input parameters, the elementary effects would vary in the input space  $\Omega^K$ . As a result,  $\hat{\sigma}_k$  is larger than 0. The scale ratio  $\hat{\sigma}_k/\hat{\mu}_k$  is used to decide if the  $\hat{\sigma}_k$  is close to 0 or larger than 0 by comparing  $\hat{\sigma}_k$  to  $\hat{\mu}_k$ .

Through the screening based on the Elementary Effect method, a number of  $M < K$  input parameters is identified as the relevant influential input parameters. Then the structure sensitivity is analyzed only under the uncertainty of these  $M$  influential input parameters by the Monte Carlo method for variance-based sensitivity analysis.

## 4.2 Quantitative method: the direct Monte Carlo simulation for variance-based sensitivity analysis

Variance-based sensitivity analysis is a widely used approach to quantify the influence of the  $K$  input parameters  $\mathbf{p} = [p_1, p_2, \dots, p_k, \dots, p_K]$  on the output variable  $f(\mathbf{p})$ . The direct Monte Carlo method is used for the variance-based sensitivity analysis to generate a large number of random samples to obtain numerical results without prior knowledge of the investigated structure. To reduce the number of samples, the direct Quasi Monte Carlo method is used as a sub-method of the direct Monte Carlo method [8]. It uses a Quasi random number generator, e.g., the Latin-Hypercube generator or the Sobol' generator. The Quasi random number generators are designed to generate random samples for a faster convergence. The drawback of the Latin-Hypercube generator is that its algorithm for the randomness of the input parameters is dependent on the sample size. The sample size cannot be changed without starting the simulation again from the beginning. In contrast, the Sobol' random number generator can freely



extend the sample size even after finishing the simulation [8]. Therefore, the Sobol' random number generator is used in this study to generate random samples of the input parameters according to their defined distribution functions  $\mathcal{N}$  and  $\mathcal{U}$  in Table 1.

The associated sensitivity indices for variance-based sensitivity analysis are the main effect index  $S_k$  and the total effect index  $S_{T_k}$  [5, 8]. The main effect index  $S_k$  is a quantitative measure of the direct influence of the  $k$ -th input parameter on the output variable. The total effect index  $S_{T_k}$  sums the main effect  $S_k$  and the interaction effects of the  $k$ -th input parameter with other input parameters. The analytical calculation of the main effect  $S_k$  and total effects  $S_{T_k}$  of the input parameters is not possible for complex structures such as the described beam structure. They can only be approximated by application of the Monte Carlo method.

The main effect  $S_k$  of each input parameter  $p_k$  is approximated according to the Sobol' Estimator  $\hat{S}_k = g(N, \mathbf{A}, \mathbf{B}, \mathbf{A}_B^{(k)})$  [15] as a function  $g$  of  $N$  numbers of the sampling trials and the simulation results of sampling matrices  $\mathbf{A}$ ,  $\mathbf{B}$ , and  $\mathbf{A}_B^{(k)}$ . The total effect  $S_{T_k}$  of each input parameter  $p_k$  is approximated according to the Jansen Estimator  $\hat{S}_{T_k} = h(N, \mathbf{A}, \mathbf{B}, \mathbf{A}_B^{(k)})$  [1, 16] as a function  $h$  of  $N$ ,  $\mathbf{A}$ ,  $\mathbf{B}$ , and  $\mathbf{A}_B^{(k)}$ . These two estimators are proven to work well for analyzing many different kinds of complex structures [1, 9]. The sampling steps to generate the sampling matrices  $\mathbf{A}$ ,  $\mathbf{B}$ , and  $\mathbf{A}_B^{(k)}$  for calculating the estimators are described in detail in [8].

For the estimation of  $\hat{S}_k$  and  $\hat{S}_{T_k}$  of a structure with  $K$  varied input parameters,  $2N$  simulations are carried out for  $\mathbf{A}$  and  $\mathbf{B}$  and  $N \cdot K$  simulations are carried out for  $\mathbf{A}_B^{(k)}$ . Totally, the number of the direct Monte Carlo simulations for variance-based sensitivity analysis is  $N_{\text{DMC}} = N \cdot (2 + K)$  [8].

#### 4.3 Quantitative method: the combined Monte Carlo method for variance-based sensitivity analysis

The number of the direct Monte Carlo simulations for calculating the sensitivity indices depends on the number of sampling trials  $N$  and the number of the varied input parameters  $K$ . If either  $N$  or  $K$  can be reduced, the sensitivity analysis can be more efficient. In case of not changing the random number generator, to ensure the accuracy of the sensitivity analysis, the number of sampling trials  $N$  should not be reduced. However, based on the Elementary Effect method, the varied input parameters are sorted as influential and non-influential parameters. Therefore, by combining the Elementary Effect method and the Monte Carlo method for variance-based sensitivity analysis, only the  $M$  influential input parameters are analyzed. The  $(K - M)$  non-influential input parameters are fixed at their deterministic values. In this way, the number of the combined Monte Carlo simulations is reduced to  $N_C = N_{\text{EE}} + N_{\text{CMC}} = R \cdot (1 + K) + N \cdot (2 + M)$ , with  $M < K$ , which is the sum of the number of the simulations for the Elementary Effect method  $N_{\text{EE}}$  and the number of the simulations for the direct Monte Carlo method  $N_{\text{CMC}}$  for  $M < K$  influential input parameters.

### 5 RESULTS AND COMPARISON OF RESULTS BASED ON THE DIRECT AND THE COMBINED MONTE CARLO METHOD

The simulations of the beam structure based on the direct Monte Carlo method and the combination of the Elementary Effect method and the Monte Carlo method are carried out according to the description in section 4. The results are discussed and compared in this section.

### 5.1 The screening results based on the Elementary Effect method

In this case study,  $R = 10$  base points are randomly chosen for screening the influence of the  $K = 14$  input parameters in Table 1 of the beam structure on the first lateral resonance frequency  $f_1$  from equation (2). The number of the simulations based on the Elementary Effect method is  $N_{EE} = R \cdot (1 + K) = 150$ . After the simulations, the mean  $\hat{\mu}_k$  and the standard deviation  $\hat{\sigma}_k$  of each input parameter's elementary effect are estimated according to equations (5) and (6) and illustrated in Figure 4.

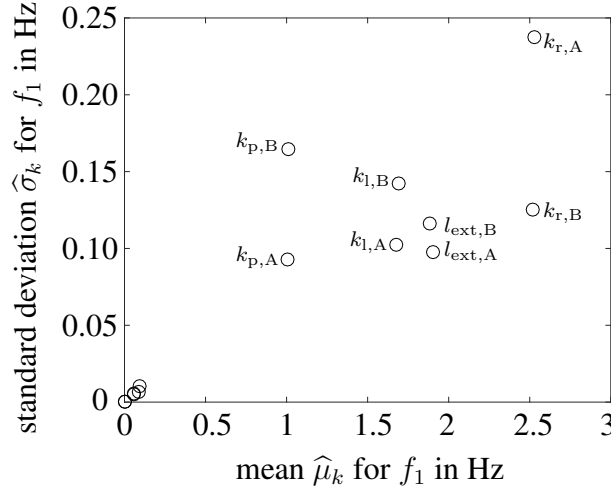


Figure 4: Screening results of the beam structure based on the Elementary Effect method

By looking at Figure 4 it can be concluded that the lateral and rotational stiffness properties of the springs  $k_{l,A}$ ,  $k_{r,A}$ ,  $k_{l,B}$ , as well as  $k_{r,B}$  and the stiffness of the piezo transducers  $k_{p,A}$  and  $k_{p,B}$  have influence on  $f_1$  when they are varied in the range shown in Table 1. The length of the axial extension on both beam ends  $l_{ext,A}$  and  $l_{ext,B}$  also affects  $f_1$ . This is seen by the high value of the mean  $\hat{\mu}_k$ . The input parameters located in the lower left corner in Figure 4 are  $E_{ext,A}$ ,  $\rho_{ext,A}$ ,  $t_{ext,A}$ ,  $E_{ext,B}$ ,  $\rho_{ext,B}$ , and  $t_{ext,B}$ . As their  $\hat{\mu}_k$  is close to 0, they do not show relevant influence on  $f_1$ . For the eight influential input parameters  $k_{l,A}$ ,  $k_{r,A}$ ,  $k_{l,B}$ ,  $k_{r,B}$ ,  $k_{p,A}$ ,  $k_{p,B}$ ,  $l_{ext,A}$ , as well as  $l_{ext,B}$ , their scale ratios  $\hat{\sigma}_k/\hat{\mu}_k$  are between 5% for  $l_{ext,A}$  and 16% for  $k_{p,B}$ . That means the standard deviation  $\hat{\sigma}_k$  of these eight input parameters is fairly small in comparison to their mean  $\hat{\mu}_k$  and implies that these eight influential input parameters' functional relations to  $f_1$  are practically linear.

According to the screening result, the  $M = 8$  input parameters  $k_{l,A}$ ,  $k_{r,A}$ ,  $k_{l,B}$ ,  $k_{r,B}$ ,  $k_{p,A}$ ,  $k_{p,B}$ ,  $l_{ext,A}$ , as well as  $l_{ext,B}$  are concluded as influential input parameters and their influences on  $f_1$  will be quantified by application of the Monte Carlo method.

### 5.2 The convergence of the sensitivity analysis results based on the direct Monte Carlo method

In this case study, the number of sampling trials is defined as  $N = 50\,000$ . Therefore, the number of the direct Monte Carlo simulations is  $N_{DMC} = N \cdot (2 + K) = 800\,000$ . The convergence of the sensitivity indices  $\hat{S}_k$  and  $\hat{S}_{T_k}$  according to the Sobol' estimator [15] and the Jansen estimator [1, 16] of each input parameter is analyzed to examine if the sample size  $N = 50\,000$  is high enough to adequately estimate the sensitivity indices  $\hat{S}_k$  and  $\hat{S}_{T_k}$ . Both sensitivity indices of each input parameter are calculated by every increase of 250 samples. In this study, all

sensitivity indices  $\hat{S}_k$  and  $\hat{S}_{T_k}$  are assumed to have converged when they stay within a variation range  $\pm 0.05$  of the value that is approximated with the sample size  $N = 50\,000$ , see the horizontal dashed lines in Figure 5. The estimated sensitivity indices of the spring rotation stiffness of the support A  $p_{10} = k_{r,A}$  by increasing the sample size  $N$  are illustrated in Figure 5 as an example.

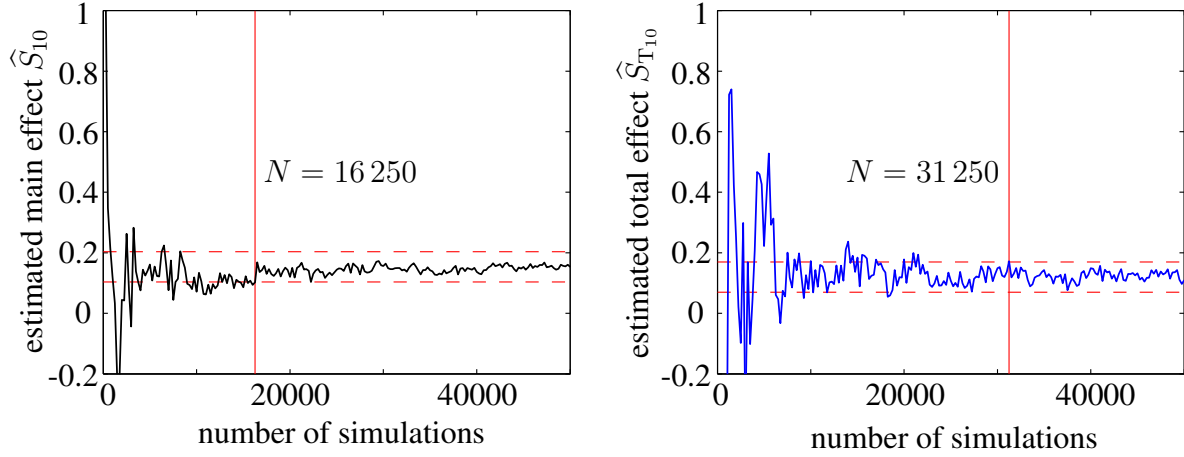


Figure 5: Convergence of sensitivity indices of  $k_{r,A}$  based on the direct Monte Carlo method

For the beam structure, the sensitivity index  $\hat{S}_{10}$  of  $p_{10} = k_{r,A}$  is converged when the estimation is based on more than  $N = 16\,250$  samples, the sensitivity index  $\hat{S}_{T_{10}}$  of  $p_{10} = k_{r,A}$  is converged when the estimation is based on more than  $N = 31\,250$  samples. These are the highest required numbers for the convergence among all  $K = 14$  input parameters in Table 1. Therefore, the sample size  $N = 50\,000$  is sufficient for the sensitivity analysis in this case study.

The values of  $\hat{S}_k$  and  $\hat{S}_{T_k}$  of each input parameter on the output variable  $f_1$  are illustrated as solid bars in Figure 7. The results are discussed and compared with the results based on the combination of the Elementary Effect method and the Monte Carlo method in section 5.4.

### 5.3 The convergence of the sensitivity analysis results based on the combined Monte Carlo method

The number of sampling trials is also defined as  $N = 50\,000$ . Therefore, the number of the combined Monte Carlo simulations is  $N_{CMD} = N \cdot (2 + M) = 500\,000$ . The same convergence analysis as for the direct Monte Carlo simulation is carried out to examine if the sample size  $N = 50\,000$  is high enough to adequately estimate the sensitivity indices  $\hat{S}_k$  and  $\hat{S}_{T_k}$ . The convergence criterion is the same as that for the direct Monte Carlo Simulation in Figure 5, sensitivity indices are assumed to have converged when they stay within a variation range  $\pm 0.05$  of the value that is, again, approximated with the sample size  $N = 50\,000$ , see the horizontal dashed lines in Figure 6. The estimated sensitivity indices  $\hat{S}_{10}$  and  $\hat{S}_{T_{10}}$  of the spring rotation stiffness of the support A  $p_{10} = k_{r,A}$  are illustrated in Figure 6 as an example.

For the beam structure, the sensitivity index  $\hat{S}_{10}$  is converged when the estimation is based on more than  $N = 9\,500$  samples, and the sensitivity index  $\hat{S}_{T_{10}}$  is converged when the estimation is based on more than  $N = 26\,500$  samples. These are the highest numbers for the convergence among the  $M = 8$  input parameters. In comparison to the direct Monte Carlo simulation, the combined Monte Carlo simulation requires a smaller number of sampling trials.

The values of  $\hat{S}_k$  and  $\hat{S}_{T_k}$  of the eight influential input parameters with  $k = 3, 7, 9, \dots, 14$

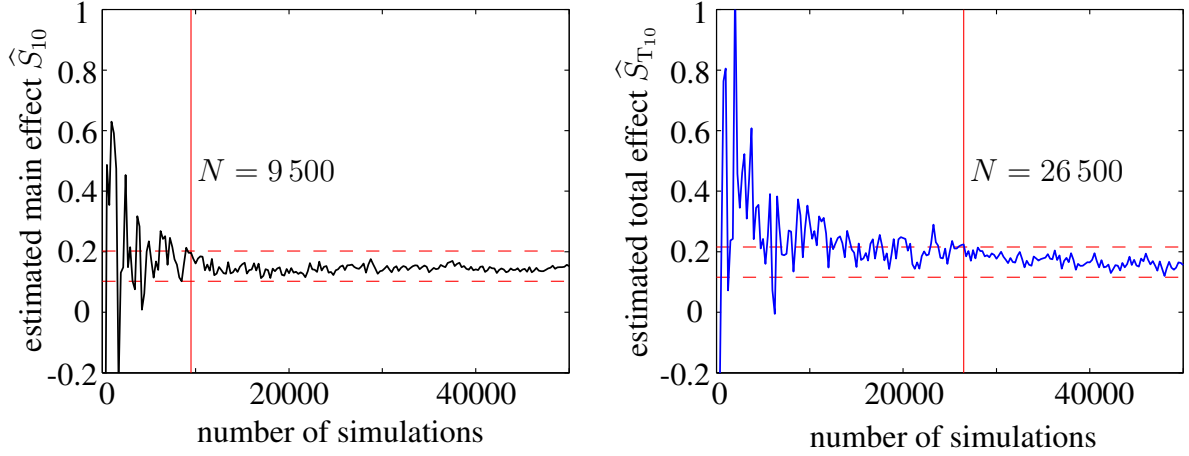
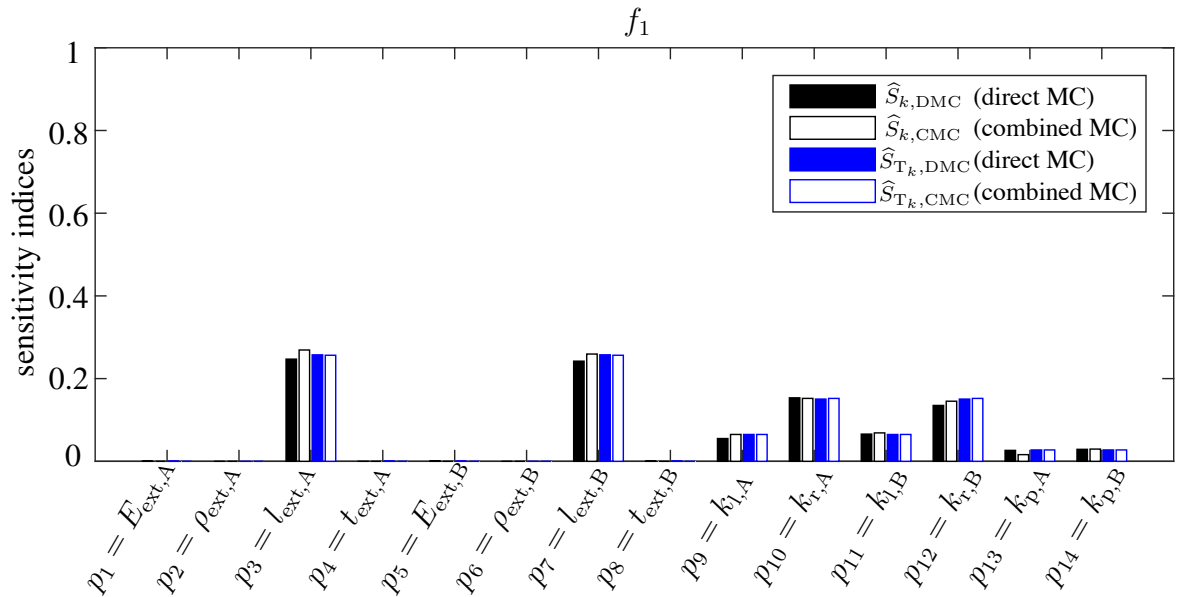


Figure 6: Convergence of sensitivity indices based on the combined Monte Carlo method

in Table 1 are illustrated as non-solid bars in Figure 7. The results are discussed and compared with the results based on the direct Monte Carlo method in section 5.4.

#### 5.4 Comparison of the results based on the direct Monte Carlo method and the combined Monte Carlo method

The sensitivity indices of the main effect  $\hat{S}_k$  and the total effect  $\hat{S}_{T_k}$  of the  $K = 14$  input parameters based on the direct Monte Carlo method and the combined Monte Carlo method based on the  $M = 8$  influential input parameters are illustrated in Figure 7.

Figure 7: Sensitivity indices  $\hat{S}_k$  and  $\hat{S}_{T_k}$  based on the direct Monte Carlo method (DMC) and the combined Monte Carlo method (CMC)

The black solid bars in Figure 7 represent the main effect  $\hat{S}_{k,\text{DMC}}$  and the blue solid bars in Figure 7 represent the total effect  $\hat{S}_{T_k,\text{DMC}}$  of the  $K = 14$  input parameters based on the direct Monte Carlo simulation. By comparing  $\hat{S}_{k,\text{DMC}}$  with  $\hat{S}_{T_k,\text{DMC}}$ , it can be observed that the value of  $\hat{S}_{k,\text{DMC}}$  is almost equal to the value of  $\hat{S}_{T_k,\text{DMC}}$  for each input parameter. It indicates that the functional relations between the input parameters and the output variable are nearly linear. This

conclusion agrees with the result based on the Elementary Effect method in section 5.1.

The estimated main and total effects  $\hat{S}_{k,\text{DMC}}$  and  $\hat{S}_{T_k,\text{DMC}}$  in Figure 7 based on the direct Monte Carlo method show that the varied input parameters  $p_3 = l_{\text{ext},A}$  and  $p_7 = l_{\text{ext},B}$  have more influence on  $f_1$  than the other varied input parameters with highest values of  $\hat{S}_{k,\text{DMC}} \approx \hat{S}_{T_k,\text{DMC}} \approx 0.25$ . Second highest are  $p_{10} = k_{r,A}$ , and  $p_{12} = k_{r,B}$  with  $\hat{S}_{k,\text{DMC}} \approx \hat{S}_{T_k,\text{DMC}} \approx 0.15$ . Third highest are  $p_9 = k_{l,A}$ ,  $p_{11} = k_{l,B}$ ,  $p_{13} = k_{p,A}$ , and  $p_{14} = k_{p,B}$  with small values of  $0.05 \leq \hat{S}_{k,\text{DMC}} \approx \hat{S}_{T_k,\text{DMC}} \leq 0.1$ . Moreover, by comparing the sensitivity indices of the input parameters of the support A and those of the support B it can be found that they are almost equal,  $\hat{S}_{3,\text{DMC}} \approx \hat{S}_{7,\text{DMC}}$ ,  $\hat{S}_{9,\text{DMC}} \approx \hat{S}_{11,\text{DMC}}$ ,  $\hat{S}_{10,\text{DMC}} \approx \hat{S}_{12,\text{DMC}}$ , and  $\hat{S}_{13,\text{DMC}} \approx \hat{S}_{14,\text{DMC}}$ . This is reasonable since the beam structure is symmetric and the two supports are built based on the same design.

The rest of the varied input parameters,  $p_1 = E_{\text{ext},A}$ ,  $p_2 = \rho_{\text{ext},A}$ ,  $p_4 = t_{\text{ext},A}$ ,  $p_5 = E_{\text{ext},B}$ ,  $p_6 = \rho_{\text{ext},B}$ , and  $p_8 = t_{\text{ext},B}$ , show no relevant influence on  $f_1$  with  $\hat{S}_{k,\text{DMC}} \approx \hat{S}_{T_k,\text{DMC}} \approx 0$ . These six input parameters are concluded as non-influential input parameters by screening based on the Elementary Effect method. Therefore, they are kept constant at their deterministic values in the combined Monte Carlo method. Their values  $\hat{S}_{k,\text{DMC}} \approx \hat{S}_{T_k,\text{DMC}} \approx 0$  indicate that none of the influential input parameters is incorrectly identified as non-influential input parameter by screening based on the Elementary Effect method.

The non-solid bars in Figure 7 represent the sensitivity indices  $\hat{S}_{k,\text{CMC}}$  and  $\hat{S}_{T_k,\text{CMC}}$  of the  $M = 8$  influential input parameters based on the combined Monte Carlo simulation.

In the visual comparison of  $\hat{S}_{k,\text{DMC}}$  and  $\hat{S}_{k,\text{CMC}}$ , as well as  $\hat{S}_{T_k,\text{DMC}}$  and  $\hat{S}_{T_k,\text{CMC}}$  in Figure 7, it can be concluded that the results based on the direct Monte Carlo method and the combined Monte Carlo method are in good agreement. To quantify the difference of the results based on these two methods, the absolute deviations of  $|\hat{S}_{k,\text{DMC}} - \hat{S}_{k,\text{CMC}}|$  and  $|\hat{S}_{T_k,\text{DMC}} - \hat{S}_{T_k,\text{CMC}}|$  of the  $M = 8$  influential input parameters are calculated. All of them are smaller than 0.01. It can be concluded that the analysis accuracy of the direct Monte Carlo method and that of the combined Monte Carlo method for variance-based sensitivity analysis is adequate.

The efficiencies of the direct Monte Carlo method and the combined Monte Carlo method for variance-based sensitivity analysis are compared according to the minimal required number of the simulations  $N_{\text{DMC},\min}$  for the direct Monte Carlo method and  $N_{\text{C},\min}$  for the combination of the Elementary Effect method and the Monte Carlo method, Table 2. It is known from the description in section 5.2 and 5.3 that the combined Monte Carlo simulation requires a lower sampling size in comparison to the direct Monte Carlo method. In this study, the sum of the minimal required number of simulations based on the direct Monte Carlo method is  $N_{\text{DMC},\min} = 500\,000$  and the sum of the minimal required number of simulations based on the combination of the Elementary Effect method and the Monte Carlo method is only  $N_{\text{C},\min} = N_{\text{EE}} + N_{\text{CMC}} = 265\,150$ . The numerical cost of the combined Monte Carlo method is only half the cost of the direct Monte Carlo method.

## 6 CONCLUSION

The combined Monte Carlo method that includes a screening of the relevant influential parameters by the Elementary Effect method was proposed as an efficient application of the Monte Carlo method to quantify structure uncertainty under input parameter uncertainty. The accuracy and the efficiency of the combined Monte Carlo method was investigated in this study by using a beam structure with piezo-elastic supports for buckling and vibration control as a reference structure. Its uncertain structural input parameters are geometric, material, and stiffness pa-

Table 2: The minimal required number of simulations based on the direct Monte Carlo method and the combined Monte Carlo method

	the direct Monte Carlo method	the combined Monte Carlo method
number of simulations for screening	0	$N_{EE} = R(1 + K)$ $= 10 \cdot (1 + 14)$ $= 150$
min. sample size for $\hat{S}_k$	16 250	9 500
min. sample size for $\hat{S}_{T_k}$	31 250	26 500
min. sample size $N_{\min}$	$N_{DMC,\min} = 31\,250$	$N_{CMC,\min} = 26\,500$
min. number of simulations for $\hat{S}_k$ and $\hat{S}_{T_k}$	$N_{DMC} = N_{DMC,\min} \cdot (2 + K)$ $= 31\,250 \cdot (2 + 14)$ $= 500\,000$	$N_{CMC} = N_{CMC,\min} \cdot (2 + M)$ $= 26\,500 \cdot (2 + 8)$ $= 265\,000$
sum of minimal number of simulations	$N_{DMC,\min} = 500\,000$	$N_{C,\min} = N_{EE} + N_{CMC}$ $= 150 + 265\,000$ $= 265\,150$

rameters of the piezo-elastic supports. The first lateral natural frequency of the beam structure is subject to be estimated as the output variable. The influence of each varied input parameter on the first lateral resonance frequency was quantified by estimated sensitivity indices. The proposed combination of the Elementary Effect method and the Monte Carlo method was compared with the direct Monte Carlo method. According to the convergence analysis, the combined Monte Carlo method required only half the number of simulations as for the direct Monte Carlo simulation in analyzing the uncertainty of the first lateral resonance frequency of the beam structure. The comparison showed that the result based on the combined Monte Carlo method is similar to the result based on the direct Monte Carlo simulation. Consequently, the combined Monte Carlo method is proven to be an efficient method for uncertainty quantification in comparison to the direct Monte Carlo simulation in the structural design phase.

### Acknowledgement

The authors would like to thank the German Research Foundation (DFG) for funding this research within the Collaborative Research Centre (SFB) 805 “Control of Uncertainties in Load-Carrying Structures in Mechanical Engineering”.

### REFERENCES

- [1] Saltelli A., Annoni P., Azzini I., Campolongo F., Ratto M., and Tarantola S., Variance based sensitivity analysis of model output. Design and estimator for the total sensitivity index. *Computer Physics Communications*, **181**, pp. 259-270, 2010.
- [2] Iooss B. and Saltelli A., Introduction to Sensitivity Analysis, *Handbook of Uncertainty Quantification*. Springer International Publishing, 2016.
- [3] Mokhatari A., Volume 1: Review of Available Methods for Conducting Sensitivity and Uncertainty Analysis in Probabilistic Models, *Review and Recommendation of Methods for Sensitivity and Uncertainty Analysis for the Stochastic Human Exposure and Dose*

- Simulation (SHEDS) Models*, report to project number 2004-206-01, prepared by Department of Civil, Construction, and Environmental Engineering, North Carolina State University for Alion Science and Technology, 2005.
- [4] Morris M. D., Factorial sampling plans for preliminary computational experiments. *Technometrics*, **33**, pp. 161-174, 1991.
  - [5] Saltelli A., et al., *Global Sensitivity Analysis: The Primer*. John Wiley & Sons, Ltd, 2008.
  - [6] Campolongo F., Cariboni J., and Saltelli A., An effective screening design for sensitivity analysis of large models. *Environmental Modelling and Software*, **22**, pp. 1509-1518, 2007.
  - [7] Zhan C., Song X., Xia J., and Tong C., An efficient integrated approach for global sensitivity analysis of hydrological model parameters. *Environmental Modelling and Software*, **42**, pp. 39-52, 2013.
  - [8] Becker W. and Saltelli A., Design for sensitivity analysis, *Handbook of Design and Analysis of Experiments*. CRC Press, 2015.
  - [9] Han S.O., *Varianzbasierte Sensitivitätsanalyse als Beitrag zur Bewertung der Zuverlässigkeit adaptiver Struktursysteme (English: Variance-based sensitivity analysis as a contribution to the assessment of reliability of smart systems)*, Ph.D. Thesis, TU Darmstadt, 2011.
  - [10] Quaglietta E. and Punzo V., Supporting the design of railway systems by means of a Sobol variance-based sensitivity analysis. *Transportation Research Part C: Emerging Technologies*, **34**, pp. 38-54, 2013.
  - [11] Schaeffner M., Götz B., and Platz R., Active buckling control of a beam-column with circular cross-section using piezoelectric supports and integral LQR control. *Smart Materials and Structures*, **25(6)**, 065008, 2016.
  - [12] Götz B., Schaeffner M., Platz R., and Melz T., Lateral vibration attenuation of a beam with circular cross-section by a support with integrated piezoelectric transducers shunted to negative capacitances. *Smart Materials and Structures*, **25(10)**, 095045, 2016.
  - [13] Enss G. C., Gehb C. M., Götz B., Melz T., Ondoua S., Platz R., and Schaeffner M., *Device for bearing design elements in lightweight structures (Festkörperlager)* Patent. DE 10 2015 101 084 A1, July 2016.
  - [14] Data sheet by PI Ceramic, Website: <https://www.piceramic.com/en/products/piezoceramic-actuators/linear-actuators/p-882-p-888-picma-stack-multilayer-piezo-actuators-100810/>, accessed on March 23, 2017
  - [15] Sobol' I.M., Global sensitivity indices for nonlinear mathematical models and their Monte Carlo estimates. *Mathematics and Computer in Simulation*, **55**, pp. 271-280, 2001.
  - [16] Jansen M. J.W., Analysis of variance designs for model output. *Computer Physics Communications*, **117**, pp. 35-43, 1999.